HHS Public Access

Author manuscript

Nat Neurosci. Author manuscript; available in PMC 2014 July 01.

Published in final edited form as:

Nat Neurosci. 2014 January ; 17(1): 106–113. doi:10.1038/nn.3582.

Prefrontal entrainment of amygdala activity signals safety in learned fear and innate anxiety

Ekaterina Likhtik[1], **Joseph M. Stujenske**[2], **Mihir A. Topiwala**[1,4], **Alexander Z. Harris**[3], and **Joshua A. Gordon**[1,4]

[1]Department of Psychiatry, College of Physicians and Surgeons, Columbia University, New York, NY, USA

[2]Department of Neuroscience, College of Physicians and Surgeons, Columbia University, New York, NY, USA

[3]Department of Psychiatry, Weill Cornell Medical College, New York, NY USA

[4]Division of Integrative Neuroscience, New York State Psychiatric Institute, New York, NY USA

Abstract

Successfully differentiating safety from danger is an essential skill for survival. While decreased activity in the medial prefrontal cortex (mPFC) is associated with fear generalization in animals and humans, the circuit level mechanisms used by the mPFC to discern safety are not clear. To answer this question, we recorded activity in the mPFC, basolateral amygdala (BLA), and dorsal (dHPC) and ventral hippocampus (vHPC) in mice during exposure to learned (differential fear conditioning) and innate (open field) anxiety. We found increased synchrony between the mPFC and BLA in the theta frequency range (4–12 Hz) only in animals that differentiate between averseness and safety. Moreover, during recognized safety across learned and innate paradigms, BLA firing becomes entrained to theta input from the mPFC. These data suggest that selective tuning of BLA firing to mPFC input provides a safety-signaling mechanism whereby the mPFC taps into the microcircuitry of the amygdala to diminish fear.

INTRODUCTION

Discriminating between aversive and safe cues is a necessary skill for survival. Fear generalization negatively impacts the ability to compete for resources in animals and is associated with a range of anxiety disorders in humans. Whereas some generalization of aversive stimuli occurs in humans as part of a normal threat assessment response[1,2], a tip in the balance toward fear generalization across a wide range of stimuli is a hallmark of learned and innate anxiety disorders, typified by post-traumatic-stress-disorder[3] (PTSD) and generalized anxiety disorder, respectively[4,5] (GAD). Clarifying the neural mechanisims

Author Contributions

E.L. designed and performed the experiments, analyzed the data and wrote the paper. J.M.S. analyzed the data. M.A.T. assisted in performing the experiments. A.Z.H. assisted in analyzing the data. J.A.G. designed the experiments, supervised the performance of the experiments and data analysis, and wrote the paper.

underlying fear discrimination and generalization is therefore key to understanding these disorders.

The mPFC has emerged as a principal candidate for top-down regulation of fear responses[6] and impulse control[7]. Indeed, a decrement in fear is associated with increased activity in the mPFC as measured by cell firing[8], local field potentials[9], activation of immediate early genes[10,11], and blood oxygenation levels[12].

Nevertheless, the mPFC is also recruited in states of high fear and anxiety. For instance, the dense projection it receives from the BLA, a critical site for fear processing, likely activates the mPFC during fear expression. In keeping with this idea, it has been shown that mPFC cell firing to conditioned tones is significantly decreased after BLA inactivation[13]. The mPFC also receives a dense projection from the vHPC[14], which is the likely source of mPFC recruitment during periods of increased innate anxiety[15, 16, 17, 18, 19].

Thus the mPFC, via its widely distributed outputs to multiple levels of the fear and anxiety circuit[20, 21, 22], is in a unique position to gate fear discrimination and threat assessment during both fear expression and suppression[13]. One mechanism the mPFC uses for long-range communication with its subcortical targets is the theta range (4–12 Hz) oscillation. Evidence shows that the mPFC, BLA and hippocampus use theta oscillations to communicate during and after fear conditioning[23, 24] as well as during extinction of conditioned fear[9] and during innate fear states[15]. These findings leave open the question how these structures dynamically interact as a network to differentiate anxiogenic and safe states.

To address these issues, and to evaluate the function of this network during fear generalization and discrimination, we simultaneously recorded activity in the BLA, mPFC, vHPC and dHPC during the recall phase of a differential fear conditioning task, and in the open field test of innate anxiety. In support of previous findings[9,23,24], theta-frequency power and synchrony in the mPFC-BLA circuit increased during high fear states. Intriguingly, synchrony in this circuit was associated with discrimination between aversive and safe cues in both tasks. Indeed, changing dynamics within the mPFC-BLA circuit accompanied successful discrimination, as captured by the directionality of theta-frequency synchrony: safety stimuli induced BLA entrainment to theta inputs from the mPFC in both tasks. We conclude that mPFC input to the BLA is a key factor governing discriminative fear learning and anxiolysis.

RESULTS

Conditioned stimuli induce theta-frequency responses in BLA, mPFC

To examine interactions between the BLA and mPFC in learned fear, animals were trained and tested in a fear discrimination task. Training consisted of three differential fear conditioning sessions. Auditory conditioning stimuli (CSs,each consisting of 30 pure-tone or white noise pips, 50 ms in duration, delivered at 1 Hz for 30 s) were paired with a mild (0.4 mA) shock to the paws (CS+) or explicitly unpaired (CS−). Five CS+ and five CS− were delivered in a pseudorandom order daily over three successive days (Fig. 1a). Recall of the

conditioned responses was tested in a novel context on the fourth day. During recall, mice consistently froze to the CS+, but varied considerably in their freezing to the CS−. Some animals froze to the CS+ and CS− equally, indicating generalization of fear, whereas others froze more to the CS+ than the CS−, suggesting that they discriminated the fear-associated CS+ from the neutral CS−. We used both continuous and dichotomous measures to classify the extent to which animals differentiated the CS+ and CS−. To quantify relative freezing to the two stimuli on a continuous basis, we used a Discrimination Score (DS), subtracting percent freezing to the CS− from percent freezing to the CS+. In our sample animals that generalized across stimuli froze to the CS− up to 10% more than the CS+. We therefore reasoned that freezing up to 10% more to the CS+ than the CS− (Supplementary Fig. 1a, grey area, DS=10) was also within the range of fear generalization. A DS of 10 also represents a reasonable midpoint between roughly two distribution peaks (Fig. 1c). Thus, to conduct a dichotomous analysis where required, those at DS ≤10 were classified as Generalizers (n=12), while animals at DS > 10 were classified as Discriminators (n=17, Fig. 1b,c). Note that Generalizers learned the cue-shock association, showing the same levels of elevated freezing to both stimuli during the recall session (Generalizers CS+, 59 ± 0.063%, CS−, 58 ± 0.06% freezing), while Discriminators froze significantly more to the CS+ (53.2 ± 0.05%) than the CS− (34.8 ± 0.04 %) (Fig. 1d and Supplementary Fig.1). To eliminate any artificial differences introduced by grouping animals, we perform both dichotomous and continuous measure analyses.

Local field potentials (LFPs) from the mPFC, BLA, dHPC and vHPC, as well as multi- and single-unit activity from the BLA were recorded during the recall test session on day 4 (Supplementary Fig. 2). Each pip evoked a field potential response in all the recorded structures with prominent delta- (1–4 Hz) and theta-frequency (4–12 Hz) components (Fig. 2a,b). Previous work has shown an increase in theta power in the amygdala in anticipation of noxious stimuli[25], as well as in the amygdala during presentations of a tone CS+[23], and during sleep following fear conditioning[24]. Consistent with these findings, we found strong pip-evoked (50–300 ms) changes in theta power during both CS+ and CS− in all regions, but only in the BLA and mPFC of Discriminators were the pip-evoked increases in theta power larger during the CS+ than the CS−. In Generalizers, theta power increased in the BLA and mPFC equally during the CS+ and CS− (Fig. 2c–e, signrank, $p>0.05$). Given that stimulus-dependent theta modulation in fear discrimination was limited to the BLA and mPFC (Supplementary Fig. 3), further analyses concentrated on these two sites. Theta power fluctuations were not purely due to differences in locomotion between groups because the same changes in theta power were found when the analysis was restricted to epochs of low speed (0–5 cm/sec, Supplementary Fig. 4). Additionally, analyses of theta BLA and mPFC theta power and coherence by speed did not yield any significant correlations (Supplementary Fig. 4). On a continuous basis, differential (CS+ − CS−) pip-evoked theta correlated with DS across the entire sample in the BLA, and trended toward significance in the mPFC (Fig. 2f, BLA, n=23, R=0.56, p=<0.01; PFC, n=27, r=0.37, p=0.06, Spearman correlation), suggesting that these increases in theta power were behaviorally relevant. The higher theta power signal during the CS+ lasted for up to 200 ms after pip onset in the BLA and up to 300 ms after pip onset in the mPFC (Fig. 2e). Finally, pip-evoked increases in theta power in the BLA and mPFC were correlated with each other (Supplementary Fig. 4,

r=0.7, p=2.8 $\times 10^{-4}$), suggesting the possibility that these increases reflected an increase in functional connectivity between the two structures.

Theta synchrony in the BLA-mPFC pathway and fear discrimination

Given the importance of theta-frequency oscillations in long-range synchrony within the HPC/BLA/mPFC circuit during fear and anxiety[9, 23,24], we examined whether the pip-evoked increases in theta power were accompanied by increases in theta-frequency synchrony between the BLA and mPFC, and whether such synchrony was modulated by CS type. To this end, pip-evoked coherence was calculated to evaluate the moment-by-moment synchrony across LFPs recorded from the BLA and mPFC. Together these results point to a dynamic, behaviorally-relevant modulation of theta synchrony between the BLA and mPFC.

Analyses of theta coherence within this circuit suggested a striking relationship between BLA-mPFC synchrony and the dynamic evaluation of threat. In Generalizers, theta-frequency coherence between the BLA and mPFC was not significantly affected by either CS (Fig. 3 a,b, n=9, CS+ median, −0.008,CS− median, 0.001, signrank, p>0.05). In Discriminators, both CSs increased theta coherence (Fig. 3b, n=13, signrank, p<0.05), and the CS+ pips elicited higher theta coherence than the CS− pips (Fig. 3b,c, CS+ median, 0.038, CS− median, 0.016, signrank, p<0.01,). This difference was not related to freezing per se because the Generalizers, a group that froze during the CS+ and CS−, did not show an increase in pip-evoked coherence above baseline for either stimulus type (Fig. 3b,c). Indeed, BLA-mPFC coherence increased as a function of discrimination (R=0.52, p<0.05, Fig. 3c). Subtraction coherograms revealed increased theta coherence during the CS+ compared to the CS− in Discriminators for up to 300 ms after pip onset (Fig. 3d, signrank, p<0.05), similar to the time course of stimulus-evoked theta power changes (Fig. 2e). Intriguingly, these data demonstrate a pip-evoked increase in theta-frequency synchrony between the BLA and mPFC during both the CS+ and CS−, but only when animals successfully learn the distinction between the aversive CS+ and the neutral CS− (Supplementary, Fig. 5). These findings suggest that the BLA-mPFC circuit is engaged after successful acquisition of differential fear conditioning, and is involved in dynamically evaluating the behavioral significance of either conditioned stimulus.

LFP recordings are susceptible to volume conduction, raising questions as to the origin of theta-frequency oscillations, particularly in the BLA, which is relatively close the hippocampus. To address this issue, we recorded multi-unit-activity (MUA) in the BLA. In keeping with the critical role the BLA plays in processing fear conditioned stimuli[26], pips evoked a firing rate increase during both the CS+ and CS− (Supplementary Fig. 5). As illustrated in Figures 4a–b, BLA spikes tend to occur more frequently near the trough of the mPFC theta oscillation. The strength of this “phase-locking” was assessed using the mean resultant length (MRL) statistic, a measure of circular concentration (see Methods). In Generalizers, phase-locking did not increase above pre-tone baseline during either stimulus (Fig. 4c). By contrast, Discriminators showed significantly higher BLA phase locking to mPFC theta during presentations of both CSs than at baseline (Fig. 4c). These findings are consistent with the coherence data, reinforcing the notion that the BLA and mPFC work together to dynamically evaluate threat signals.

Learned anxiety: mPFC leads the BLA during the CS−

Our results suggest that the BLA and mPFC use theta oscillations as a means of long-range communication for successful threat evaluation. However, the highly reciprocal connectivity between these areas precludes any anatomical inferences about the direction of information transfer between them. We therefore examined the temporal relationship of BLA phase locking to mPFC theta in Generalizers and Discriminators during stimulus presentation. Directionality is inferred by determining the lag at which phase-locking of BLA MUA to mPFC theta tends to be maximal; if, for example, BLA activity is best phase-locked to the mPFC LFP of the past, we infer that the predominant directionality is from the mPFC to the BLA[27,16]. In Generalizers, BLA MUA did not have a preferential temporal relationship with mPFC theta during either stimulus, suggesting equal influence in both directions (Supplementary Fig. 5). In Discriminators, directionality depended upon CS type. During the aversive CS+, again no net directionality was found (n=24, signrank, $p>0.05$). During the neutral CS−, however, the BLA MUA had a statistically significant tendency to phase-lock best to the mPFC of the past (Fig. 4d, bottom panels, n=26, −27.5 ms, signrank, $p<0.01$), suggesting a predominant mPFC-to-BLA directionality. Importantly, Discriminators showed a significant shift (n=22, signrank, $p=0.011$) in directionality from the CS+ (no net directionality) to the CS− (mPFC lead), whereas Generalizers did not have such a switch (n=11, signrank, $p=0.4$).

To confirm these findings from the BLA MUA, we examined directionality using well-isolated BLA single units (n=25, 8 mice, see Methods for inclusion criteria). The firing of one such BLA unit and a simultaneously occurring mPFC theta oscillation is shown in Figure 4e, showing a similar phase locking profile to mPFC theta as in the MUA recordings. Insufficient numbers of spikes were obtained to conduct a lag analysis on each of the 25 single units. However, since most of the single units tended to phase-lock best to similar theta phases (near the trough, or zero phase) we were able to pool the single units and conduct an aggregate directionality analysis (Fig. 4f). The aggregate analysis revealed the same temporal pattern of activity as did the MUA. During presentations of the CS− to the Discriminator group, BLA single units (n=12, 4 mice) were significantly more phase locked to mPFC theta of the recent past than to mPFC theta of the near future (Fig. 4f, blue line, −200–0ms, −.28±0.2, versus 0–200 ms, 0.24±.02, signrank, $p=.018$). These same units, however, did not exhibit a significant difference in phase locking between past and future during presentations of the CS+ (Fig. 4f, red line, −200–0ms, −.25±0.01, versus 0–200 ms, 0.25±.02, signrank, $p>0.05$). Single units (n=13, 4 mice) recorded from Generalizers did not demonstrate a preferred lag during either stimulus type (Fig. 4f, inset, CS−, −200–0 ms, 0.27±.02, 0–200ms, 0.28±.03, signrank, $p>0.05$; CS+, −200–0ms, 0.22±.01, 0–200ms, 0.23±.01, signrank, $p>0.05$).

To evaluate mPFC-BLA directionality on a continuous basis, we performed a trial by trial analysis of directionality[28]. Because unit data requires large numbers of spikes to estimate directionality, we instead calculated mean lag times from the cross-correlation of theta power between LFPs recorded from the BLA and mPFC (Fig 5a). Specifically, we analyzed the probability of an mPFC lead as a function of percent freezing on any given trial (Fig. 5b,c). This analysis showed that whereas for Discriminators the probability of an mPFC lead

on a given trial was negatively correlated with percent freezing (Fig. 5d; multiple linear regression; CS+: R= −0.57, p<0.001, CS−: R= −0.60, p<0.001), there was no such correlation for the Generalizers (Supplementary, Fig. 5; multiple linear regression; CS+ and CS−: p>0.05). Indeed, on a continuous scale of discrimination, increased probability of an mPFC lead during the CS− (Fig. 5b), was associated with better discrimination (Fig. 5e, R= −0.578, p<0.01). Together these data argue strongly for a direct relationship between a predominant mPFC-to-BLA directionality, and suppression of freezing behavior during successful fear discrimination.

Innate anxiety: mPFC leads the BLA in safe zones

Conditioned, anxiogenic stimuli functionally elevate and modulate the theta oscillation in the BLA-mPFC circuit. Neutral stimuli, when recognized as such, shift the directionality of mPFC-BLA communication toward an mPFC-to-BLA direction of information transfer. To test whether this shift in communication is task specific or a hallmark of a broader safety recognition mechanism, we turned to the open field (Supplementary Fig. 6), a classic test of innate anxiety[29]. In this task, we first exposed animals to a small, dark familiar environment for 10 minute sessions over four days. On the fourth day, we also placed the animals in a brightly lit (185 lux) open field (Supplementary, Fig. 6a). This task taps into the innate avoidance of bright, open spaces displayed by rodents; the level of anxiety elicited by the open field is determined by the amount of time spent in the center of the field, with less center time indicating more anxiety. Supplementary Figure 6a shows an example of an animal's movement in the open field with periphery movement shown in blue and center movement shown in red. Notably, although the same animals were exposed to learned and innate anxiety tasks, there was no correlation between anxiety level in the open field and DS in fear conditioning (r=0.183, p>0.05).

In agreement with the aversive conditioned stimulus data shown above, theta power in the BLA increased with innate anxiety in the open field. We have previously demonstrated similar changes in mPFC and vHPC theta power in this task[15]. The more anxious an animal tended to be, the more BLA theta increased on the open field, especially in the relative safety of the periphery (Fig. 6a, n=14, r= −0.42, p<0.05). We therefore reasoned that theta synchrony between the two regions might also increase in this task. Indeed, using theta power correlations, we found that BLA-mPFC theta synchrony increased with anxiety in the periphery of the open field (n=14, r= −0.52, p<0.05,. 6b). Notably, increased BLA-mPFC synchrony in the open field was not due to novelty. BLA-mPFC power correlations, similar to the mPFC-vHPC circuit[15], were also significantly higher in the open field compared to the first familiar environment exposure (Supplementary, Fig.7).

BLA theta modulation by innate anxiety led us to examine whether BLA firing within the open field also differs with anxiety. To this end animals were divided into two groups, Anxious (n=9, spending <10% of their time in the center, and Non-anxious (n=5), showing >10% center time in the open field, Supplementary, Fig. 6b). It should be noted that whereas "Non-anxious" refers to little evidence of anxiety, such that animals are not actively seeking the safety of the periphery, "Generalizers" in learned fear refers to generalized defensive behavior to both CSs.

Notably, BLA firing rates of Anxious animals increased as they moved away from the periphery and into the center of the open field, whereas in the Non-anxious animals BLA firing rates did not change with radial distance (multiple linear regression, anxious: $R= -0.6344$, $p<.001$; non-anxious: $R= -0.3294$, $p >0.05$, Fig. 6c,d). Intriguingly, in Anxious animals, as BLA firing decreased in the periphery of the open field, mPFC theta power and mPFC - BLA coherence increased (Fig. 6e,f). Thus, when the Anxious animals are in the periphery of the open field, BLA and mPFC theta power and synchrony increases whereas BLA neural firing decreases.

To investigate these relationships further, we analyzed the transitions as animals shuttled between the periphery and the center. In Anxious animals, BLA firing rates increased only as they transitioned into the center from the periphery (Fig.7a). Indeed, as Anxious animals moved from the periphery into the center, BLA and mPFC theta power as well as BLA-mPFC field-field and spike-field coherence decreased (Fig. 7c,e) until they reentered the periphery, when mPFC power and mPFC-BLA synchrony went back up again (Fig. 7d,f). In Non-anxious animals these changes were not observed (Supplementary, Fig. 8a,b). These data indicate that an innate anxiety component contributes to BLA spiking as Anxious animals are going toward the center. On the contrary, when an Anxious animal is headed toward the relative safety of the periphery, the mPFC signal increases in power and synchrony with the BLA, and the BLA firing rate decreases.

Finally, we examined the effect of the open field on directionality within the circuit using power correlation lag[28] and phase-locking lag[16,27] analyses. An analysis of BLA MUA phase locking to the mPFC LFP showed that, consistent with the findings in the fear conditioning task, when Anxious animals were in the safety of the periphery, spiking in the BLA was best phase locked to the mPFC theta oscillation of the past (Fig. 8,$n= 30$, -15 ms, signrank, $p<0.01$). Notably, this relationship was absent when Anxious animals were in the anxiogenic center of the open field (Fig. 8, $n=30$, signrank, $p>0.05$). BLA MUA from Non-anxious animals did not show any net directionality in either location (Supplementary Fig. 8c, signrank, $p>0.05$). These findings demonstrate a similar relationship between BLA spiking and the mPFC theta oscillation in conditioned and innate anxiety. Namely, when an animal evaluates a potentially anxiogenic situation and detects safety (be it a neutral CS or a safe zone in an aversive environment), BLA spiking shifts to following theta input from the mPFC (Fig. 8).

Discussion

We investigated the dynamic interactions of the mPFC-BLA-hippocampal network in learned fear and innate anxiety. While CS–evoked responses were found throughout the network, mPFC-BLA interactions were specifically enhanced during successful fear discrimination. Theta-frequency synchrony between the mPFC and BLA was enhanced by both CSs in animals that successfully discriminated between a CS+ and CS−; similarly, enhancements in mPFC-BLA synchrony correlated with center-avoidance in the open field test. In both environments, safety was accompanied by a net mPFC-to-BLA directionality. These data demonstrate that the mPFC-BLA circuit is dynamically engaged in fear discrimination, and suggest that the mPFC inputs to the BLA are involved in actively

squelching behavioral responses to fear by entraining activity within the BLA to mPFC theta input.

The mPFC is widely accepted as a critical site for inhibition of fear in human anxiety and in animal models of PTSD[30] and GAD[6]. The amygdala is a hub of fear responding and a centralized site for the prefrontal cortex to control for fear decrement. The anxiolytic role for the mPFC has been most widely studied using extinction of conditioned fear in animals and humans, where findings converge to show that increased mPFC activity and cortical volume correspond with better and longer lasting extinction in experimental and clinical settings[8, 31]. Indeed, extinction training is one of the most widely used techniques for overcoming fear in clinical practice[32]. Our findings are consistent with the notion that the mPFC-BLA circuit is a key player in diminishing fear and anxiety[33, 34], and extend the role of the mPFC and the mPFC-BLA circuit from fear extinction to fear discrimination showing that mPFC-BLA interactions partake in the appraisal of safety versus averseness.

mPFC inputs and microcircuits of the amygdala

Our data demonstrate a distinct mPFC-to-BLA directionality during fear discrimination. Our findings suggest that the mPFC relies on this projection to shape activity in the BLA during fear discrimination, possibly resulting in inhibition of amygdala output. The fact that during fear discrimination BLA cells are entrained to theta input from the mPFC is likely due to the interplay between this input and intrinsic currents of BLA neurons, which predispose them to oscillate in the theta range[35]. Anatomically, a robust mPFC-to-BLA projection has been described, with most mPFC axon terminals synapsing on dendritic spines of BLA projection neurons, and only a few terminating on putative interneurons[36]. How this predominantly excitatory-to-excitatory projection[37] results in a fear decrement (which presumably requires inhibition of amygdala output), is unclear. Given that GABAergic transmission in the BLA is key to reducing fear[38, 39, 40, 41], it may be that tuning into theta-encoded input from the mPFC allows for the activation of a subset of local inhibitory networks in the amygdala. Indeed, *GAD65*$^{-/-}$ mice have been shown to generalize fear early in extinction training and show decreased theta communication between the mPFC and amygdala[42].

To this end, discrimination might rely on similar mechanisms as fear extinction. Indeed, prefrontal theta has been shown to increase during extinction training[9] and there is mPFC-dependent inhibition of fear output cells in the central nucleus of the amygdala[43] (CE). This is associated with increased efficacy of the mPFC-to-BLA synapse, which in turn may activate CE-projecting GABAergic cell clusters in the amygdala known as the intercalated (ITC) cell masses[43]. Indeed, evidence in rats and mice shows that ITC cells are active during and required for extinction[44, 45].

Safety across paradigms

Our findings show that BLA firing is tuned to mPFC input in recognized safety across fear discrimination and innate anxiety, suggesting that this is a widely used mechanism for safety detection. This idea supports previous work showing that BLA cells active after extinction are responsive to stimulation of the mPFC[34]. Critically, this mechanism was only engaged in animals that identified safety as either a cue (CS−) or a location (periphery of open field) in

an otherwise aversive setting. During CS+ presentations there was higher theta power and sharper theta reset (Supplementary, Fig. 9) seen in the BLA and mPFC, suggesting that there is an additional fear related input. During recognized safety, this common input is likely decreasing, diminishing theta power in these areas, and allowing for the mPFC to influence activity in the BLA. Importantly, this mechanism was not engaged in animals that generalized fear across the two stimuli or were not anxious in the open field.

A growing literature suggests that it is the infralimbic cortex (IL) rather than the more dorsal prelimbic cortex (PL) of the mPFC that plays a role in fear decrement[12, 46, 47]. Most of our recordings were performed in the PL, with some on the PL/IL border. We did not see any differences in our results based on electrode placement. However, given that we were recording LFPs in two contiguous areas, we cannot rule out that the relatively slow theta oscillation of the mPFC was volume conducted from one subregion of the mPFC to another.

These data support a unified view of forebrain fear and anxiety circuitry in safety detection (Supplementary, Fig. 10). In the conditioned fear discrimination and innate anxiety, the mPFC and BLA appear to work together to evaluate behaviorally-relevant stimuli; for safe stimuli, the mPFC drives BLA activity, inhibiting fear. In this way the dynamics of cooperation and competition with the mPFC-BLA circuit determine the expression of fear- and anxiety-related behaviors.

Methods

The procedures described here were conducted in accordance with National Institutes of Health regulations and approved by the Columbia University and New York State Psychiatric Institute Institutional Animal Care and Use Committees.

Microdrive Construction

Custom microdrives were constructed using interface boards (EIB-16, Neuralynx, Bozeman, MT) fastened to machine screws (SHCX-080-6, Small Parts, Inc, Miramar, FL). Stereotrodes (4–5 per animal) were constructed of 25 μM Formvar-coated tungsten micro wire (California Fine Wire, Grover Beach, CA), fastened to a cannula attached to the interface board, and implanted in the BLA. Single-wire, 76.2 μM tungsten electrodes were stereotactically placed into the dHPC, vHPC and mPFC and cemented directly to the skull during surgery.

Surgery

Three- to six-month-old male 129Sv/Ev wild-type mice (Taconic, Germantown, NY) were initially anaesthetized with ketamine/xylazine (160 and 5.5 mg/kg, in saline), placed in a stereotaxic frame (Kopf Instruments, Tujunga, CA) and maintained on inhaled isoflurane (0.5 – 0.8%) in oxygen for the duration of the surgery. Temperature was monitored and maintained at 36.6°C with a feedback regulated heating pad. The skull was leveled using bregma and lambda landmarks and craniotomies were made using anterior-posterior (AP) coordinates from bregma, medo-lateral (ML) coordinates from the midline and dorso-ventral coordinates (DV) from brain surface. Stereotrodes were implanted in the BLA (−2.06 mm AP, 3.15 mm ML, −3.4 mm DV) and tungsten wires were placed into the dorsal CA1 of the

hippocampus (dHPC: −1.85 mm AP, 1.25 mm ML and −1.15 mm DV), the medial prefrontal cortex (mPFC: +1.65 mm AP, 0.3 mm ML, −1.6 mm DV) and the ventral hippocampus (vHPC, −3.16 mm AP, 3.0 mm ML, −3.7 mm DV). Skull screws overlying the cerebellum and frontal cortex served as ground and reference, respectively. All wires were connected to a 16-channel interface and the BLA electrodes were anchored to a microdrive that made it possible to advance them along the DV axis. Postoperatively, animals were given analgesics (Carpofen, 5 mg/kg, s.c.) and monitored for comfort and weight gain. Following surgery, animals were housed individually on a 12 hour light/dark cycle, with bedding squares provided for enrichment.

Behavioral Protocol

Innate Anxiety—Animals recovered for at least one week or until regaining pre-surgery body weight. Mice were then food restricted to 85% body weight. During food restriction animals were familiarized to the recording setup and handled by being tethered to the head stage preamplifier in their home cages for two to three daily sessions of 15 min each. All behavioral experiments were performed between 2 and 5 pm. Upon reaching their target weight, mice (n=21) were exposed to a small rectangular box ("familiar arena," 30 × 20 cm) in the dark in which they foraged for food once a day for three consecutive days (10 min per session). On the fourth day, to test innate anxiety the animals were again exposed to the familiar arena for 10 minutes and 1 hour later to a brightly lit (180 Lux) open field (25 cm radius, 40 cm high, Fig. 6A).

Differential Fear Conditioning

After three days of rest, the same animals were exposed to differential fear conditioning (1 session a day for three days) in a dimly lit (30 Lux) conditioning chamber with a grid floor of stainless steel bars for shock delivery (MedAssociates, St. Albans, VT). The animals were habituated to the context for 2–3 minutes prior to each training session and were then presented with 10 trials of tones (8 kHz, white noise, counterbalanced), 5 of which were the aversive conditioning stimulus (CS+) and co-terminated with a footshock to the paws (0.4 mA, 1 sec), and 5 of which were the neutral conditioning stimulus (CS−) and were not paired with anything. Therefore the animals received a total of 30 stimuli over three days, 15 CS+ and 15 CS−. The order of stimulus presentation was pseudorandom on all days of training and testing. Stimuli consisted of pure tone pips lasting 50 ms and delivered at 1Hz for 30 seconds (inter-trialinterval, 60–180 sec). Stimuli were randomly assigned as the CS+ and CS− and were counterbalanced between animals (Fig. 1a). On the fourth day, the animals were placed in a new context (a wooden enclosure, 60 Lux) for testing how well they had learned the differential associations with the two stimuli. The animals were connected to the recording equipment and after 2–3 minutes of habituation, presented with the same CS+ and CS− stimuli as during training. An overhead video camera was used to monitor and record the behavior of the animals for offline analysis of freezing. Freezing was manually scored twice by a trained observer blind to the valence of the tone. The two scores had to be less than two seconds apart to be averaged for a final score. To increase the number of Discriminators and thereby the power of our tests, we also tested a second group of 8 animals in differential fear conditioning using 6 trials of CS+ and CS− each session over the same three day period as in the previous group. Therefore these animals received a

total of 36 trials over three days, 18 CS+ and 18 CS−. Sample sizes were increased in order to have sufficient data for a continuous analysis as a function of discrimination and to have sufficient power when analyzed as group data (Generalizers versus Discriminators). These animals were only used in the power and coherence analyses shown in figures 2 and 3, where the effects did not differ between the groups (p=0.921, ttest).

Histology

At the end of all experiments, animals were deeply anesthetized with ketamine (180 mg/kg) and current (50 μA, 10 s) was passed through the electrodes to lesion for track verification (Supplementary Fig. 2). Animals were then perfused, brains were cut on a cryostat (60 μm) and stained for Nissl bodies using cresyl violet. Only animals with proper electrode placement were included in the analysis. One animal was excluded from the analysis because of a thalamic tumor.

Data Acquisition

Recordings were obtained via a unitary gain head-stage preamplifier (Neuralynx, Bozeman, MT) attached to a fine wire cable. Multi- and single-units were obtained by lowering stereotrodes in the BLA until well isolated units (threshold of 38 μV) were obtained. Spikes were bandpass-filtered (600 – 6000 Hz) and recorded at 32 kHz. Electrodes were lowered between the innate and learned anxiety paradigms in order to get new cells in the BLA. LFP signals from all areas were recorded against the reference screw. Field potential signals were amplified, bandpass filtered (1–1000 Hz), and acquired at 1894 Hz. Both LFP and multiunit data were acquired by a Lynx 8 programmable amplifier (Neuralynx, Bozeman, MT) on a personal computer running Cheetah data acquisition software (Neuralynx, Bozeman, MT). The animal's position was obtained by overhead video tracking of two light-emitting diodes affixed to the head stage (sampled at 30 Hz).

Data Analysis

Data was imported into Matlab (Natick, MA) for analysis. A combination of custom written scripts, and Chronux analysis package[48] (http://chronux.org) were used for the analyses. To gauge activity within and synchrony across regions during CS+ and CS− presentations we first looked at spectrograms throughout the tone presentation period. Chronux scripts were used to obtain multi-taper spectrograms with a 375 ms (710 samples) moving window, a 5 ms overlap, a time-bandwidth product of 1.5 with 2 tapers, and 1024 FFTs. This analysis showed that in accordance with previous work using pips in tone fear conditioning[49] the most pronounced physiological changes were occurring around the onset of the pips (Fig. 2a,b) and we therefore concentrated on pip-evoked changes from pretone for further investigation. Pip-evoked changes in LFP power were then quantified using a multi-taper method after initial filtering of the field potential for the theta range using a zero-phase-delay filter (filter0, provided by K. Harris and G. Buzsaki) and the power envelope extracted from the Hilbert transform of the theta-filtered signal. To verify that our findings were not due to differences in freezing, a separate power analysis was performed on data that was speed filtered for 0–5 cm/sec from each 30 second CS presentation. This speed range was chosen to include moments when the animal was freezing but had small traveling head

movements that sometimes accompany the freezing posture and which would be picked up as slow shifts in the LED tracking.

To quantify the reliability of the theta phase reset, we extracted phase information from the Hilbert transform of the theta-filtered signal and generated histograms of the phase distributions. The half-width of these circular normal distributions was calculated from the circular standard deviation. Coherence between the BLA and mPFC was calculated using multitaper coherence[48] (http://chronux.org) using a 250 ms window, 1.5 time-bandwidth product (NW), 2 tapers, and 1024 FFTs.

We also examined synchrony between areas by looking at whether BLA firing was modulated by, or phase locked to, the mPFC theta oscillation by using custom Matlab scripts along with the circular statistics toolbox. The phase of each theta-filtered sample was extracted from the Hilbert transform and each spike was assigned the phase of its contemporaneous field potential sample. Phase-locking was quantified as the circular concentration of the resulting phase distribution, which was defined as the mean resultant length (MRL) of the phase angles. The MRL is the sum of the unit vectors representing the phases at which each spike occurred, divided by the number of spikes. It therefore takes values between zero (no phase-locking) and one (perfect phase-locking). Because the MRL statistic is sensitive to spike number, the number of spikes used for the analysis was fixed at 500, which is large enough to avoid overestimating phase locking due to small spike number. Thus, only multi-units with at least 500 spikes for each pretone and each CS type were included for analysis. The MRL statistic was calculated using 500 randomly selected spikes, repeated 2000 times and the results averaged for each multi-unit.

To analyze the directionality of BLA multi-unit phase locking to mPFC theta, multi-units with at least 100 spikes in each 30 second CS period were included because the MRL statistic can be highly variable for small spike numbers. The spike times were lagged relative to the theta filtered signal from −100 ms to 100 ms, stepping by 5 ms, and the time of the peak MRL value was determined for each multi-unit. Multi-units were determined to be significantly phase-locked using a Bonferroni-corrected p-value for the Rayleigh z-test ($p<.0012$ or $p<.05/41$). The number of significantly phase-locked units did not significantly vary for different time windows or time steps, and the directionality of the mPFC-BLA interaction was consistent across different calculation parameters. The median of the peak MRL times was compared to the null hypothesis of a zero time lag using sign rank and determined to be significant for $p < .05$. For single units, cells were clustered using Klustakwik (by Ken Harris, http://klustakwik.sourceforge.net/), using the first three principal components for cluster isolation. Clusters were kept for analysis if two independent signal-to-noise ratios ≥3 and their isolation distance was ≥ 10.MRL calculations with single units were performed only on units with a firing rate of at least .1 Hz. To analyze directionality of mPFC-BLA power-power correlations[28] as a function of freezing, the raw LFP was filtered for theta (4–12 Hz, 400 sample FIR filter) and the power envelope was extracted with the Hilbert transform. Cross-correlation lag analysis was performed with 1 second windows, stepping by 5 ms. The probability of PFC, BLA, and no lead was quantified as the percentage of windows with a positive, negative, or zero lag at the peak, respectively.

For the open field analyses, theta power was calculated with Welch's power spectral density, using 1000 samples (528.262 ms), and stepping by 100 samples (52.82 ms). For the power correlations, first we calculated multi-taper theta frequency spectrograms (2.6 sec windows, NW of 2.5) across the 10 minute exposure to the familiar environment and the open field. The linear correlation coefficient between summed BLA and mPFC theta power was calculated separately for each animal and open field power fluctuations were normalized by the familiar environment. To evaluate circuit-level communication in the open field as a function of anxiety, we took animals that spent ≤10% in the center of the open field as the "Anxious" group (n=9) and all animals ≥10% center time as the "Not-anxious" group (n=6). To analyze the directionality of BLA MUA to mPFC theta, we took all significantly phase locked multi-units with at least 1000 spikes for the entire session and then performed the same lag analysis as described for the fear conditioning test. For the transitions analyses, we identified the times at which an animal moved between a radius of >16.97 cm (95 pixels) to <14.29 cm (80 pixels) from the center. Theta coherence and power at the transitions was calculated using mutlitaper spectral analysis (1024 sample window size, 2048 FFTs, stepping by 60 samples, NW of 2, 3 tapers). For the power-power correlations directionality analysis[35], we used the same parameters as in the differential fear conditioning.

Statistics

Wilcoxon's signed rank test was used for comparisons involving measurements from the same animal across behavioral conditions, such as changes in theta power to the CS+ and the CS−. Wilcoxon's ranksum (equivalent to the Mann-Whitney U-test) non-parametric tests were used for unpaired, independent observations. Two-tailed tests were used throughout. A paired ttest was used when we had a sufficiently large sample size to adequately estimate normality.

To test for significance in firing rate around transition points (time 0) in the open field (Figs. 7a,d), we compared +/−2 seconds around the transition point to a 3 second baseline prior to the transition (−5 to −2 sec). To control for Type I error we first found only those time bins that were different from baseline at a significance level that was Bonferroni corrected for the number of bins used in the analysis – "point-wise" significance - (120 bins, 33 ms each, ttest, $p<.00041$ $(0.05/120)$)[50]. The point-wise significance level is indicated by a darker line in Fig. 7a. We then tested only those bins that were contiguous with the "point-wise" significant bins for "global" significance ($p<0.05$)[50]. The "global significance" is indicated by a lighter line in Fig. 7a. Therefore, the "globally significant" data only comes from data that is also "point-wise" significant. Similarly, to test for significance in theta power changes around the transition point, the Wilcoxon signrank test was performed on the +/−2 seconds around the transition and compared to 3 seconds of baseline. "Point-wise" significance (Figs. 7c,f, darker significance line) was achieved only when two bins in a row were $p<.0039$ different from baseline (maximal signrank significance, n=9 [Anxious animals]). To assess "global" significance (Figs. 7c,f, lighter significance colors), we took bins with $p<0.05$ significance only if they were contiguous with bins that were "point-wise" significant.

We used non-parametric tests because we test ratios, which are not normally distributed; percentages, which have floor and ceiling effects; and circular statistics, such as the Rayleigh test, to assess significance of phase locking. Analyses of means and/or medians ± standard errors of means (±SEMs) were calculated and plotted to show the accuracy of the estimation of the mean of the population. Degrees of freedom are n−1 throughout. For the continuous analyses, Pearson's correlation statistics were used unless otherwise stated. For correlations with multiple data points per animal, multiple linear regression was performed in Matlab (regstats function), including categorical variables corresponding to animal identities to account for within-animal dependence along with the explanatory variables of interest.

Supplementary Material

Refer to Web version on PubMed Central for supplementary material.

Acknowledgements

We would like to thank T. Spellman and other members of the Gordon lab for technical assistance and thoughtful discussion. This work was supported by grants from the NIMH to J.A.G (R01 MH081968 and P50 MH096891) and E.L. (F32 MH088103), by the International Mental Health Research Organization (J.A.G.), and by the Charles H. Revson Foundation (E.L.). J.M.S. is supported through the Columbia University Medical Scientist Training Program.

References

1. Resnik J, Sobel N, Paz R. Auditory aversive learning increases discrimination thresholds. Nat. Neurosci. 2011; 14:791–796. [PubMed: 21552275]
2. Dunsmoor JE, Mitroff SR, LaBar KS. Generalization of conditioned fear along a dimension of increasing fear intensity. Learn. Memory. 2009; 16:460–469.
3. Jovanovic T, Kazama A, Bachevalier J, Davis M. Impaired safety signal learning may be a biomarker of PTSD. Neuropharmacology. 2012; 62:695–704. [PubMed: 21377482]
4. Reinecke A, Becker ES, Hoyer J, Rinck M. Generalized implicit fear associations in generalized anxiety disorder. Depress. Anxiety. 2010; 27:252–259. [PubMed: 20112248]
5. Gazendam FJ, Kamphuis JH, Kindt M. Deficient safety learning characterizes high trait anxiety individuals. Biol Psychol. 2013; 92:342–352. [PubMed: 23174693]
6. Greenberg T, Carlson JM, Cha J, Hajcak G, Mujica-Parodi LR. Ventromeidal prefrontal cortex reactivity is altered in generalized anxiety disorder during fear generalization. Depress. Anxiety. 2012
7. Narayanan NS, Horst NK, Laubach M. Reversible inactivations of rat medial prefrontal cortex impair the ability to wait for a stimulus. Neurosci. 2006; 139:865–876.
8. Burgos-Robles A, Vidal-Gonzalez I, Santini E, Quirk GJ. Consolidation of fear extinction requires NMDA receptor-dependent bursting in the ventromedial prefrontal cortex. Neuron. 2007; 53:871–880. [PubMed: 17359921]
9. Lesting J, Narayanan RT, Kluge C, Sangha S, Seidenbecher T, Pape HC. Patterns of coupled theta activity in amygdala-hippocampal-prefrontal cortical circuits during fear extinction. PLoS One. 2011 Jun 28. published online.
10. Knapska E, Maren S. Reciprocal patterns of c-Fos expression in the medial prefrontal cortex and amygdala after extinction and renewal of conditioned fear. Learn. Mem. 2009; 16:486–493. [PubMed: 19633138]
11. Herry C, Mons N. Resistance to extinction is associated with impaired immediate early gene induction in medial prefrontal cortex and amygdala. Eur. J. Neurosci. 2004; 20:781–790. [PubMed: 15255988]

12. Phelps EA, Delgado MR, Nearing KI, LeDoux JE. Extinction learning in humans: role of the amygdala and vmPFC. Neuron. 2004; 43:897–905. [PubMed: 15363399]
13. Sotres-Bayon F, Sierra-Mercado D, Pardila-Delgado E, Quirk GJ. Gating of fear in prelimbic cortex by hippocampal and amygdala inputs. Neuron. 2012; 76:804–812. [PubMed: 23177964]
14. Jay TM, Witter MP. Distribution of hippocampal CA1 and subicular efferents in the prefrontal cortex of the rat studied by means of anterograde transport of Phaseolus vulgaris-leucoagglutinin. J. Comp. Neurol. 1991; 313:574–586. [PubMed: 1783682]
15. Adhikari A, Topiwala MA, Gordon JA. Synchronized activity between the ventral hippocampus and the medial prefrontal cortex during anxiety. Neuron. 2010; 65:257–269. [PubMed: 20152131]
16. Adhikari A, Topiwala MA, Gordon JA. Single units in the medial prefrontal cortex with anxiety-related firing patterns are preferentially influenced by ventral hippocampal activity. Neuron. 2011; 71:898–910. [PubMed: 21903082]
17. Bannerman DM, Gubb M, Deacon RM, Yee BK, Feldon J, Rawlins JN. Ventral hippocampal lesions affect anxiety but not spatial learning. Behav. Brain. Res. 2013; 139:197–213. [PubMed: 12642189]
18. Gordon JA, Lacefield CO, Kentros CG, Hen R. State-dependent alterations in hippocampal oscillations in serotonin 1A receptor-deficient mice. J. Neurosci. 2005; 25:6509–6519. [PubMed: 16014712]
19. Kjelstrup KG, Tuvnes FA, Steffenach HA, Murison R, Moser EI, Moser MB. Reduced fear expression after lesions of the ventral hippocampus. Proc. Natl. Acad. Sci. U.S.A. 2002; 99:10825–18030. [PubMed: 12149439]
20. Sesack SR, Deutch AY, Roth RH, Bunney BS. Topographical organization of the efferent projections of the medial prefrontal cortex in the rat: an anterograde tract-tracing study with Phaseolus vulgaris leucoagglutinin. J. Comp. Neurol. 1989; 290:213–242. [PubMed: 2592611]
21. Vertes RP. Differential projections of the infralimbic and prelimbic cortex in the rat. Synapse. 2004; 51:32–58. [PubMed: 14579424]
22. Carmichael ST, Price JL. Limbic connections of the orbital and medial prefrontal cortex in macaque monkeys. J. Comp. Neurol. 1995; 363:615–641. [PubMed: 8847421]
23. Seidenbecher T, Laxmi TR, Stork O, Pape HC. Amygdalar and hippocampal theta rhythm synchronization during fear memory retrieval. Science. 2003; 301:846–850. [PubMed: 12907806]
24. Popa D, Duvarci S, Popescu AT, Léna C, Paré D. Coherent amygdalocortical theta promotes fear memory consolidation during paradoxical sleep. Proc. Natl. Acad. Sci. U.S.A. 2010; 107:6516–6519. [PubMed: 20332204]
25. Paré D, Collins DR. Neuronal correlates of fear in the lateral amygdala: multiple extracellular recordings in conscious cats. J. Neurosci. 2000; 20:2701–2710. [PubMed: 10729351]
26. LeDoux JE. Emotion circuits in the brain. Annu. Rev. Neurosci. 2000; 23:155–184. [PubMed: 10845062]
27. Siapas AG, Lubenov EV, Wilson MA. Prefrontal phase locking to hippocampal theta oscillations. Neuron. 2005; 46:141–151. [PubMed: 15820700]
28. Adhikai A, Sigurdsson T, Topiwala MA, Gordon JA. Cross-correlations of instantaneous amplitudes of field potential oscillations: a straightforward method to estimate the directionality and lag between brain areas. J. Neurosci. Methods. 2010; 191:191–200. [PubMed: 20600317]
29. Crawley JN. Exploratory behavior models of anxiety in mice. Neurosci. Biobehav. Rev. 1985; 9:37–44. [PubMed: 2858080]
30. Rauch SL, Shin LM, Phelps EA. Neurocircuitry models of posttraumatic stress disorder and extinction: human neuroimaging research-past, present, and future. Biol. Psychiatry. 2006; 60:376–382. [PubMed: 16919525]
31. Milad MR, Quinn BT, Pitman RK, Orr SP, Fischl B, Rauch SL. Thickness of ventromedial prefrontal cortex in humans is correlated with extinction memory. Proc. Natl. Acad. Sci. U.S.A. 2005; 102:10706–10711. [PubMed: 16024728]
32. Hauner KK, Mineka S, Voss JL, Paller KA. Exposure therapy triggers lasting reorganization of neural fear processing. Proc. Natl. Acad. Sci. U.S.A. 2012; 109:9203–9209. [PubMed: 22623532]
33. Paré D, Pape HC. Plastic synaptic networks of the amygdala for the acquisition, expression, and extinction of conditioned fear. Physiol. Rev. 2010; 90:419–463. [PubMed: 20393190]

34. Herry C, Ciocchi S, Senn V, Demmou L, Müller C, Lüthi A. Switcthing on and off fear by distinct neuronal circuits. Nature. 2008; 454:600–606. [PubMed: 18615015]
35. Pape HC, Paré D, Driesang RB. Two types of intrinsic oscillations in neurons of the lateral and basolateral nuclei of the amygdala. J. Neurophysiol. 1998; 79:205–216. [PubMed: 9425192]
36. Brinley-Reed M, Mascagni F, McDonald AJ. Synaptology of prefrontal cortical projections to the basolateral amygdala: an electron microscopic study in the rat. Neurosci. Lett. 1995; 202:45–48. [PubMed: 8787827]
37. Likhtik E, Pelletier JG, Paz R, Paré D. Prefrontal control of the amygdala. J. Neurosci. 2005; 25:7429–7437. [PubMed: 16093394]
38. Truitt WA, Johnson PL, Dietrich AD, Fitz SD, Shekhar A. Anxiety-like behavior is modulated by a discrete subpopulation of interneurons in the basolateral amygdala. Neurosci. 2009; 160:284–294.
39. Woodruff AR, Sah P. Inhibition and synchronization of basal amygdala principal neuron spiking by parvalbumin-positive interneurons. J. Neurophysiol. 2007; 98:2956–2961. [PubMed: 17715201]
40. Shaban H, Humeau Y, Herry C, Cassasus G, Shigemoto R, Ciocchi S, Barbieri S, van der Putten H, Kaupmann K, Bettler B, Lüthi A. Generalization of amygdala LTP and conditioned fear in the absence of presynaptic inhibition. Nat Neurosci. 2006; 9:1028–1035. [PubMed: 16819521]
41. Heldt SA, Mou L, Ressler KJ. In vivo knockdown of GAD67 in the amygdala disrupts fear extinction and the anxiolytic-like effect of diazepam in mice. Transl. Psychiatry. 2012 Nov 13. published online.
42. Sangha S, Narayanan RT, Bergado-Acosta JR, Stork O, Seidenbecher T, Pape HC. Deficiency of the 65 kDa isoform of glutamic acid decarboxylase impairs extinction of cued but not contextual fear memory. J. Neurosci. 2009; 29:15713–15720. [PubMed: 20016086]
43. Amano T, Unal CT, Paré D. Synaptic correlates of fear extinction in the amygdala. Nat. Neurosci. 2010; 13:489–494. [PubMed: 20208529]
44. Busti D, Geracitano R, Whittle N, Dalezios Y, Maríko M, Kaufmann W, Sätzler K, Singewald N, Capogna M, Ferraguti F. Different fear states engage distinct networks within the intercalated cell clusters of the amygdala. J. Neurosc.i. 2011; 31:5131–5144.
45. Likhtik E, Popa D, Apergis-Schoute J, Fidacaro GA, Paré D. Amygdala intercalated neurons are required for expression of fear extinction. Nature. 2008; 454:642–645. [PubMed: 18615014]
46. Vidal-Gonzalez I, Vidal-Gonzalez B, Rauch SL, Quirk GJ. Microstimulation reveals opposing influences of prelimbic and infralimbic cortex on the expression of conditioned fear. Learn. Mem. 2006; 13:728–733. [PubMed: 17142302]
47. Laurent V, Westbrook RJ. Inactivation of the infralimbic but not the prelimbic cortex impairs consolidation and retrieval of fear extinction. Learn. Mem. 2009; 16:520–529. [PubMed: 19706835]
48. Mitra, P.; Bokil, H. Observed Brain Dynamics. New York: Oxford University Press; 2008.
49. Rogan MT, Stäubli UV, LeDoux JE. Fear conditioning induces associative long-term potentiation in the amgydala. Nature. 1997; 390:604–607. [PubMed: 9403688]
50. Fujisawa S, Amarasingham A, Harrison MT, Buzsáki G. Behavior-dependent short-term assembly dynamics in the medial prefrontal cortex. Nat Neurosci. 2008; 11:823–833. [PubMed: 18516033]

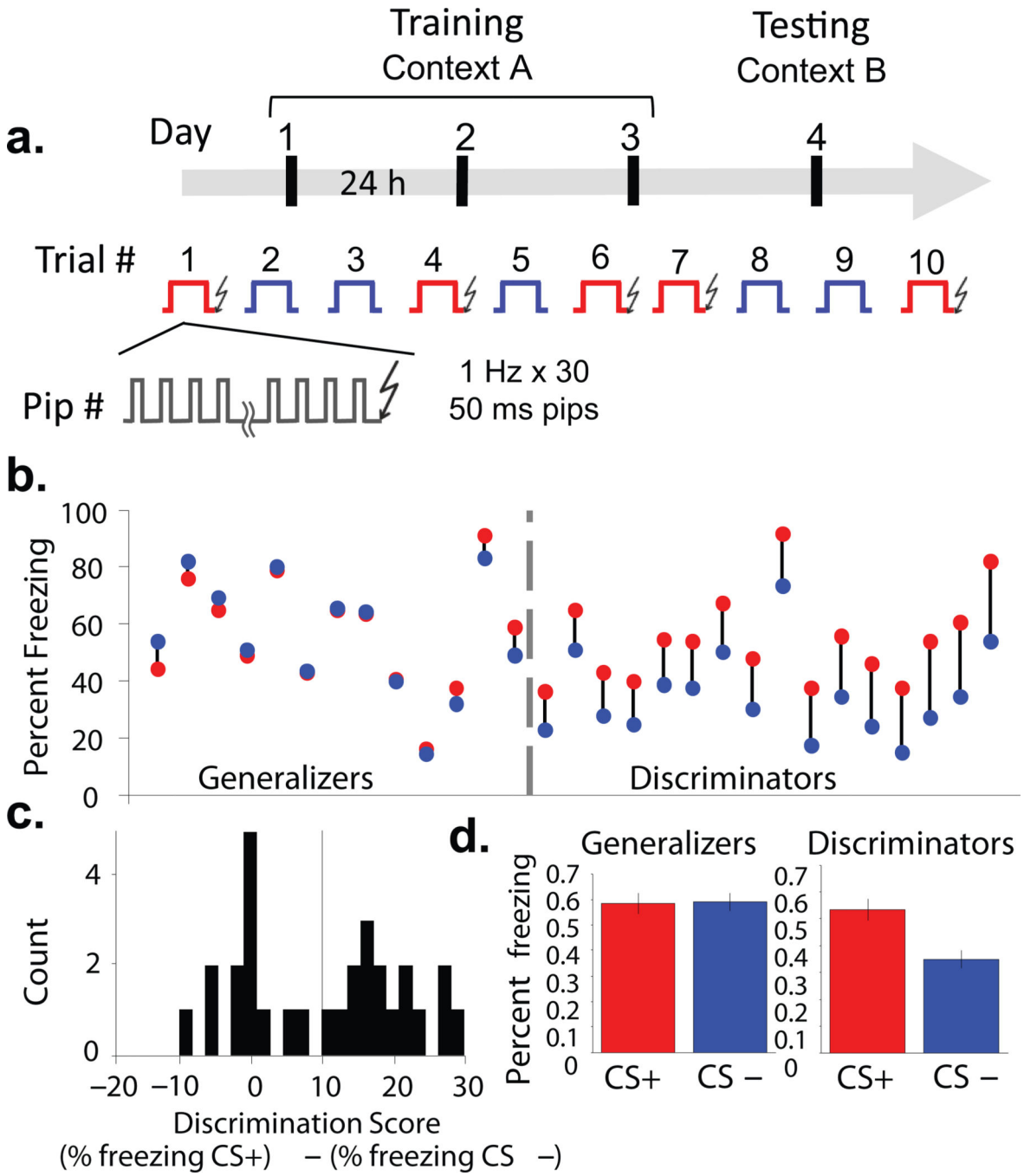

Figure 1. Individual variation in discrimination after differential fear conditioning

(**a**) Experimental protocol. Over three successive days, mice were exposed to five presentations each of a CS+ (red) or CS− (blue). Each stimulus consisted of 30 pips, 50 ms in duration, presented at 1 Hz. Each presentation of the CS+ was paired with a 1 s shock. On the fourth day, freezing responses to five additional presentations each of the CS− and CS+ were assessed in the absence of shock. (**b**) Individual animals' freezing to CS+ (red circles) and CS− (blue circles). (**c**) Histogram of discrimination scores in the sample; vertical line,

cutoff for discrimination (**d**) Freezing to CS+ and CS− for Generalizers (left) and Discriminators (right), (mean +/− s.e.m.).

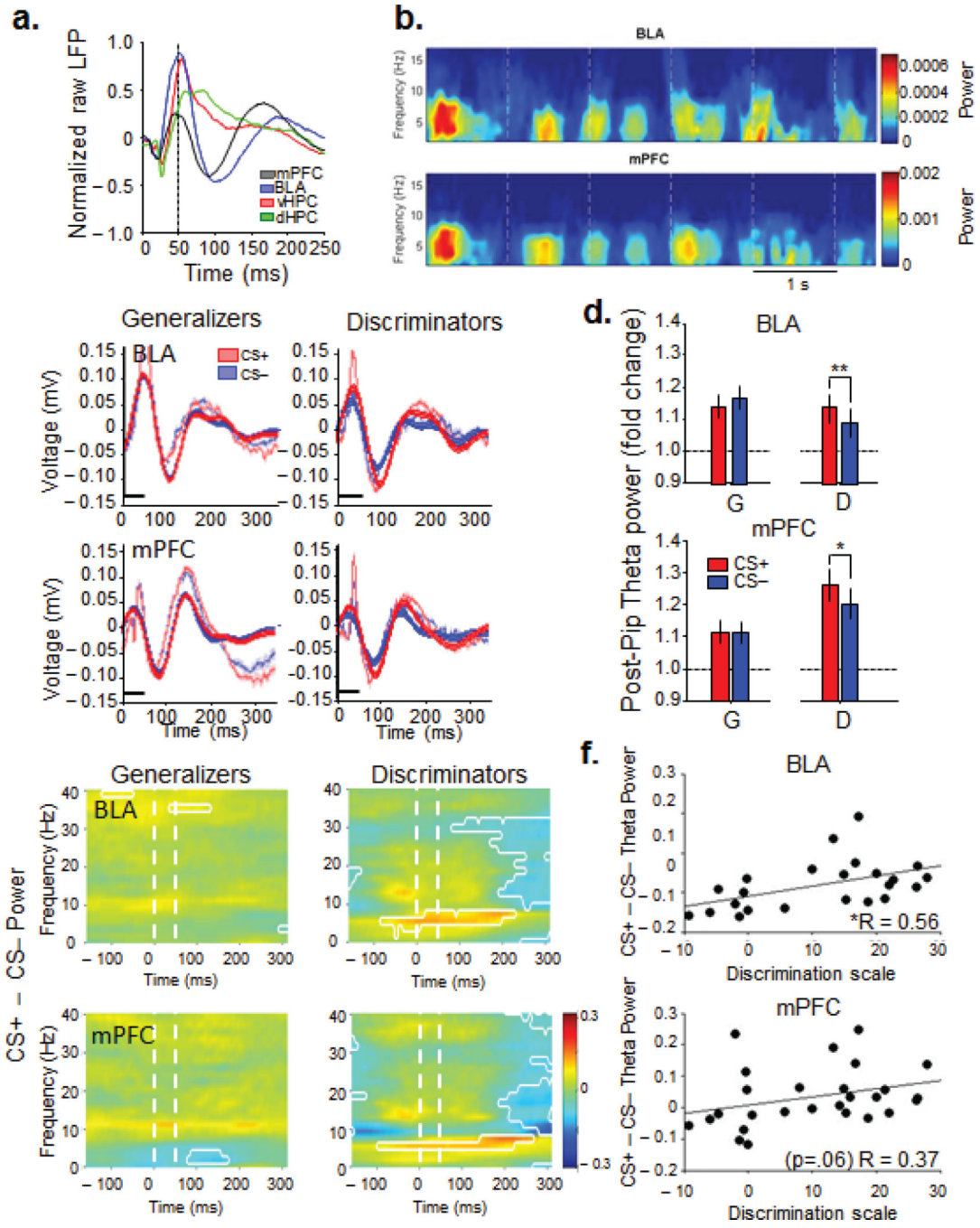

Figure 2. Pip-evoked responses in amygdala and mPFC are modulated by successful discrimination

(**a**) Example pip-evoked LFP in mPFC, BLA, vHPC and dHPC. Mean of 145 pip presentations from a single animal. Dashed line, pip offset (**b**) Example spectrogram of BLA and mPFC pip responses. Dashed lines,pip onset. (**c**) Examples of averaged (faded) and theta-filtered average (solid) traces +/− sem (faded bands) of CS+ and CS− pip-evoked responses from Generalizers and Discriminators. Black line, 50ms pip presentation. (**d**) Pip-induced change in theta power by CS type and area for Generalizers (G) and Discriminators

(D). Mean +/− s.e.m, Generalizers: BLA: n=8,CS+,1.14±.04, CS−, 1.17±.04, signrank, p>0.05; Discriminators: BLA, n=13, CS+, 1.14±.04, CS−, 1.09±.04, signrank, p<0.05; Generalizers: mPFC, n=12, CS+,1.12±.04, CS−, 1.12±.03, signrank, p>0.05, Discriminators: mPFC, n=14, CS+, 1.26±.05, CS−, 1.20±.05, signrank, p<0.05 (**e**) Subtractive spectrograms of pip-evoked power. The difference between power evoked by the CS+ and the CS− is shown as a function of frequency and time relative to each pip. Warm colors: CS+ > CS−. Cool colors, CS− > CS+. Significant ($p < 0.05$) power differences are circumscribed by white lines. 50 consecutive significant windows were required for significance. (**f**) Changes in pip-evoked theta power from the CS− to the CS+ are correlated with Discrimination Score (BLA, R=0.56, p<.05; mPFC, R=0.37, p=.06).

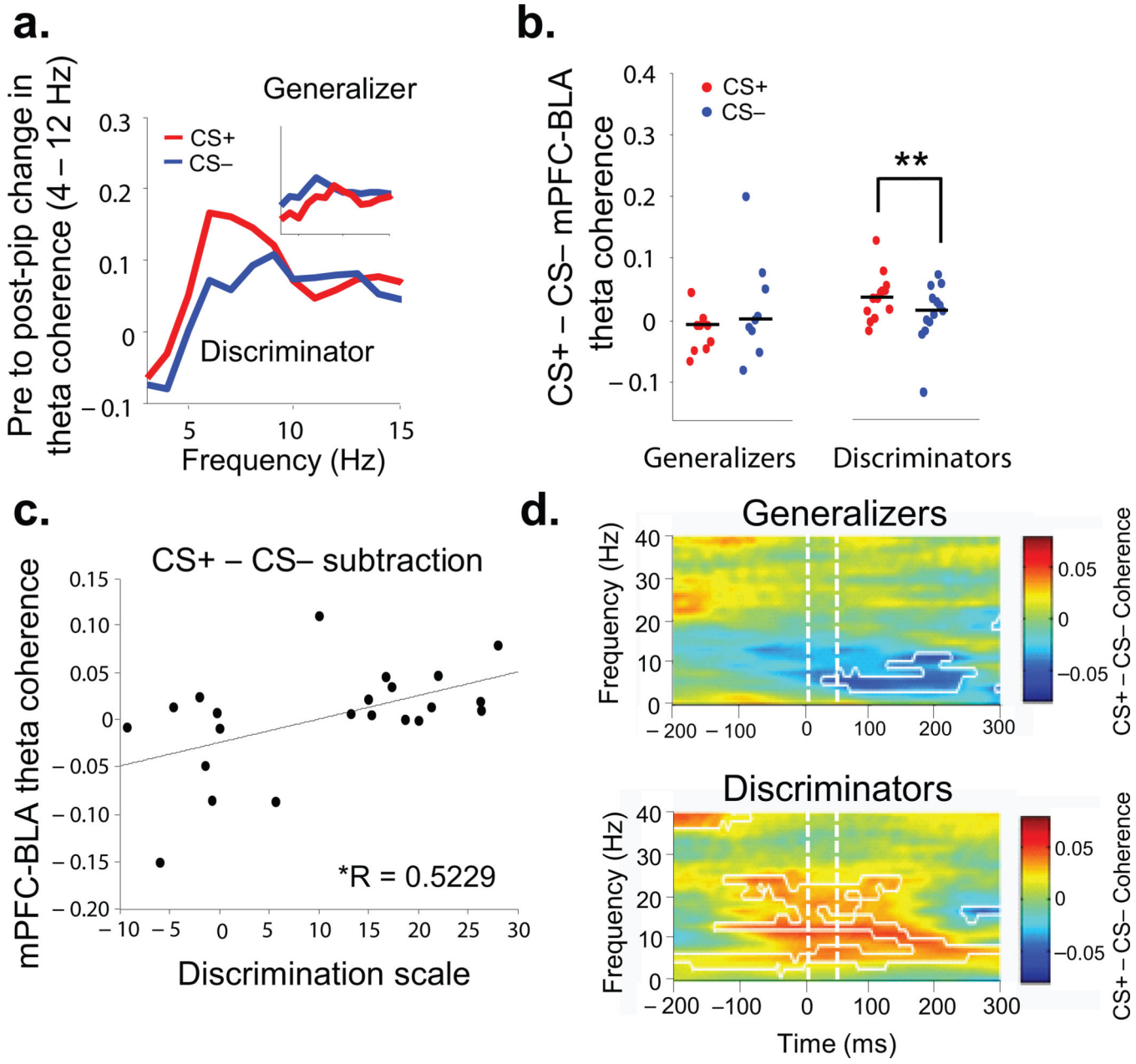

Figure 3. Enhanced BLA-mPFC synchrony after successful fear discrimination

(**a**) Pip-evoked change in theta-frequency coherence in an example Discriminator by stimulus type. Inset, same in example Generalizer. (**b**) Medians and distribution of pip-evoked changes in theta-frequency coherence for all Generalizers and Discriminators, by stimulus type. (**c**) Changes (CS− to CS+) in mPFC-BLA theta coherence are correlated with Discrimination Score (R=0.5229, p<.05) (**d**) Subtractive coherograms of pip-evoked coherence. Conventions as in Figure 2e.

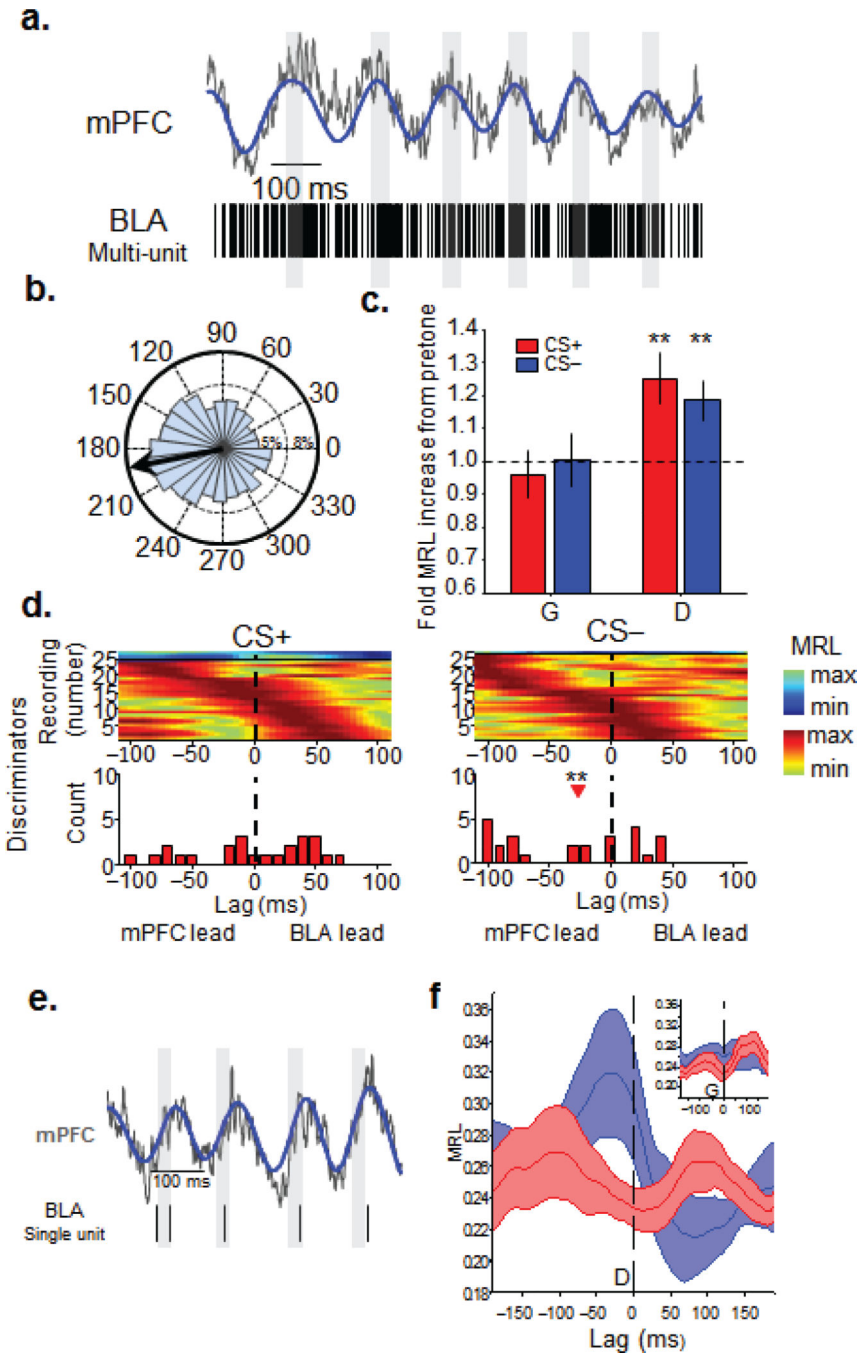

Figure 4. The CS− is associated with mPFC-to-BLA directionality in discriminators

(**a**) Example raw (grey) and theta-filtered (blue) mPFC LFP traces, along with simultaneously recorded multiunit activity recorded in the BLA. Grey bars are aligned on zero phase. (**b**) Distribution and mean (black arrow) of theta phases from this recording. (**c**) Fold increase in the strength of MUA phase-locking in Generalizers (G) and Discriminators by stimulus type. (Generalizers, CS+ (n=24), 0.96 ± 0.07, signrank, p>0.05; CS− (n=24), 1.00 ± 0.08, signrank, p>0.05, Discriminators, fold increase in MRL from pre-tone to CS+, n=29, 1.25±0.08, signrank, p=<0.01; CS− (n=29), 1.19±0.06, signrank, p=<0.01) Mean +/−

s.e.m. **, $p < 0.01$. (**d**) Color plots are phase locking strength as a function of lag for all multiunit recordings from Discriminators, aligned by peak lag and grouped by significance of phase-locking (cool colors, n.s.; warm colors, $p < 0.05$). Histograms below each plot are distributions of lags at which peak phase-locking occurred for significant units only. Red arrowhead indicates median lag that is significantly different from 0. **, $p < 0.01$ (**e**) Example raw and theta-filtered mPFC LFP and simultaneously recorded BLA single unit activity. Conventions as in Figure 4a. (**f**) Mean (solid lines) +/− s.e.m. (faded bands) phase locking strength averaged across all single units recorded from Discriminators, as a function of lag, grouped by stimulus type. Inset, same for all single units recorded from Generalizers. During the CS−, BLA single units of Discriminators (blue line, n=12), were significantly more phase locked to mPFC theta oscillations of the recent past than the near future (200-0ms versus 0–200 ms, signrank, p=.018).

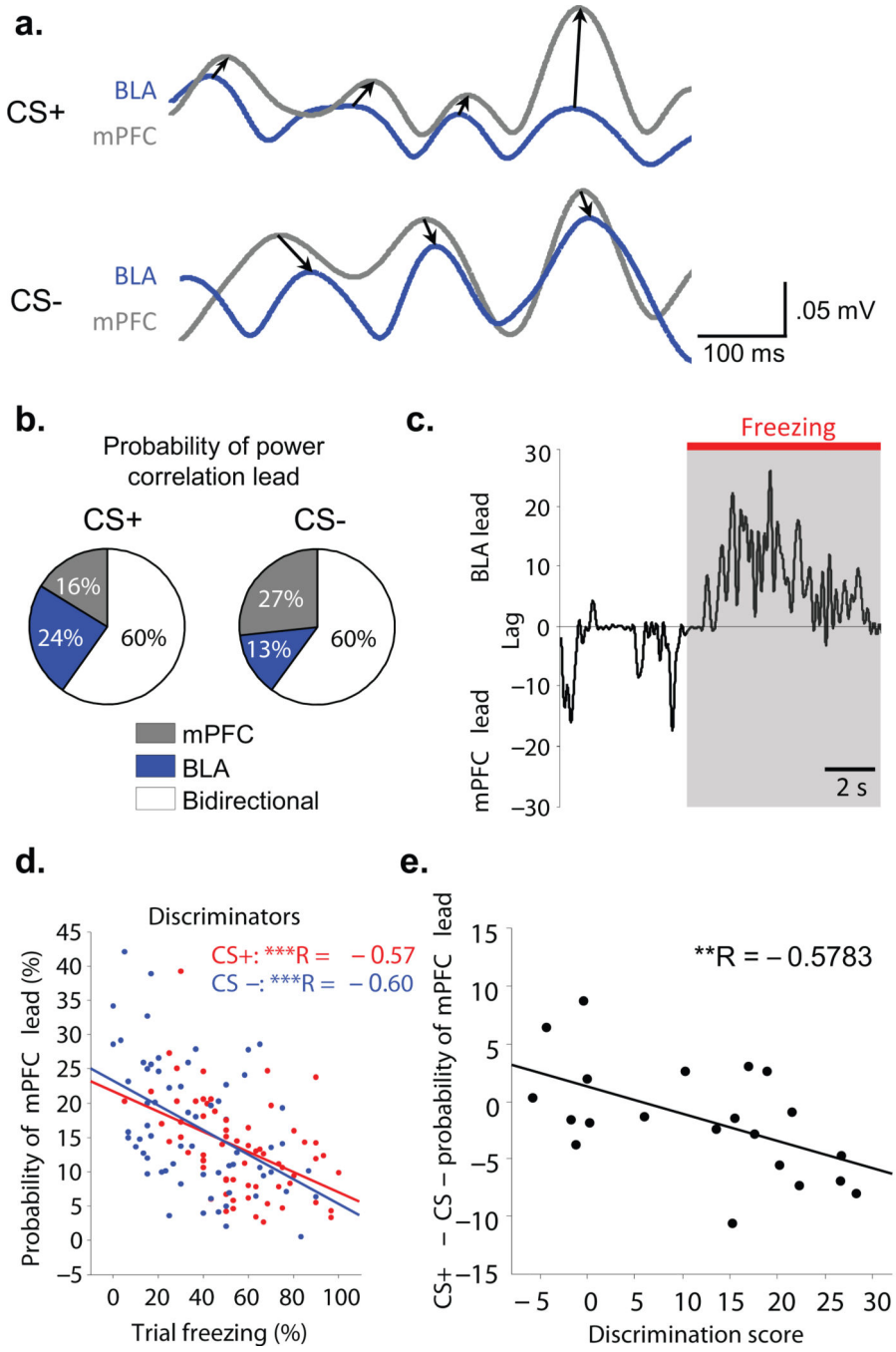

Figure 5. Short time scale fluctuations in mPFC-lead are associated with Discrimination

(**a**) Examples of BLA and mPFC theta filtered recordings illustrating the power cross-correlation lag analysis in the CS+ (top) and CS− (bottom). Arrows drawn from the leading area to the lagging area (**b**) Example of a discriminator showing that the proportion of time with an mPFC lead in the power correlation increases in CS− (average across 5 CS+ and 5 CS− trials). (**c**) Fine scale switches in power lead/lag correlations. Within trial example showing that an increased BLA lead is associated with freezing, whereas increased mPFC lead occurs during movement. (**d**) Discriminators show a negative correlation between the

proportion of time the mPFC leads and percent freezing on a given trial. (CS+, R= −0.57, p<.001; CS−, R= −0.6, p<.001). (**e**) Correlation between the change (CS+ − CS−) in the probability of an mPFC lead and Discrimination Score (R = −0.5783, p<.01). A larger mPFC lead in the CS− occurs at higher Discrimination scores.

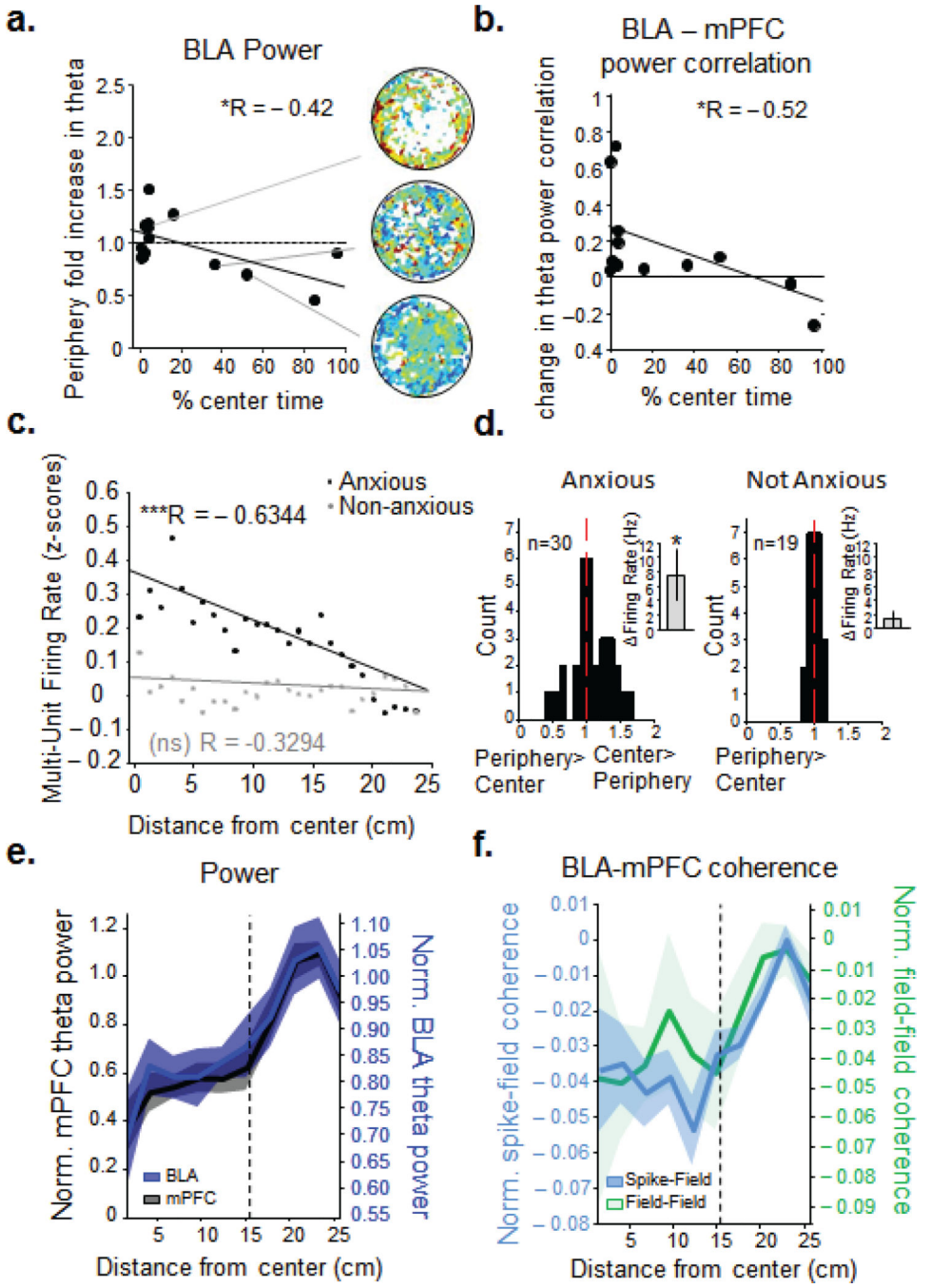

Figure 6. BLA synchronizes with mPFC in the periphery and increases firing in the center of the open field

(**a**) Fold increase in BLA theta power (compared to familiar environment) and (b) change in theta power correlation between BLA and mPFC as a function of center avoidance in the open field. *, $p < 0.05$, **, $p < 0.01$ for linear correlation (black line). (**c**) BLA firing rate as a function of Distance from the center on the open field for Anxious (black, R= − 0.6344, p<.001) and Non-Anxious animals (grey, R=− 0.3294, p>.05) (**d**) Fold change in BLA spike rate in center compared to periphery for multiunit recordings from Anxious (left) and Non-

Anxious (right) animals. Firing rate increased by 7.55 ± 3.53 Hz (paired ttest, $p<0.05$) for the Anxious animals (left inset), whereas it did not change for the Non-Anxious animals (right inset, 1.33 ± 1.23 Hz increase, paired ttest, $p>0.05$) (**e**) In Anxious animals, normalized mean mPFC (black line) and BLA (blue line) theta power **f** increase as they travel from the center to the periphery of the open field. (**f**) Anxious animals' normalized BLA spike- mPFC field (blue line, left axis) and BLA field- mPFC field (green line, right axis) coherence increase with the distance from the center (faded bands, +/− sem).

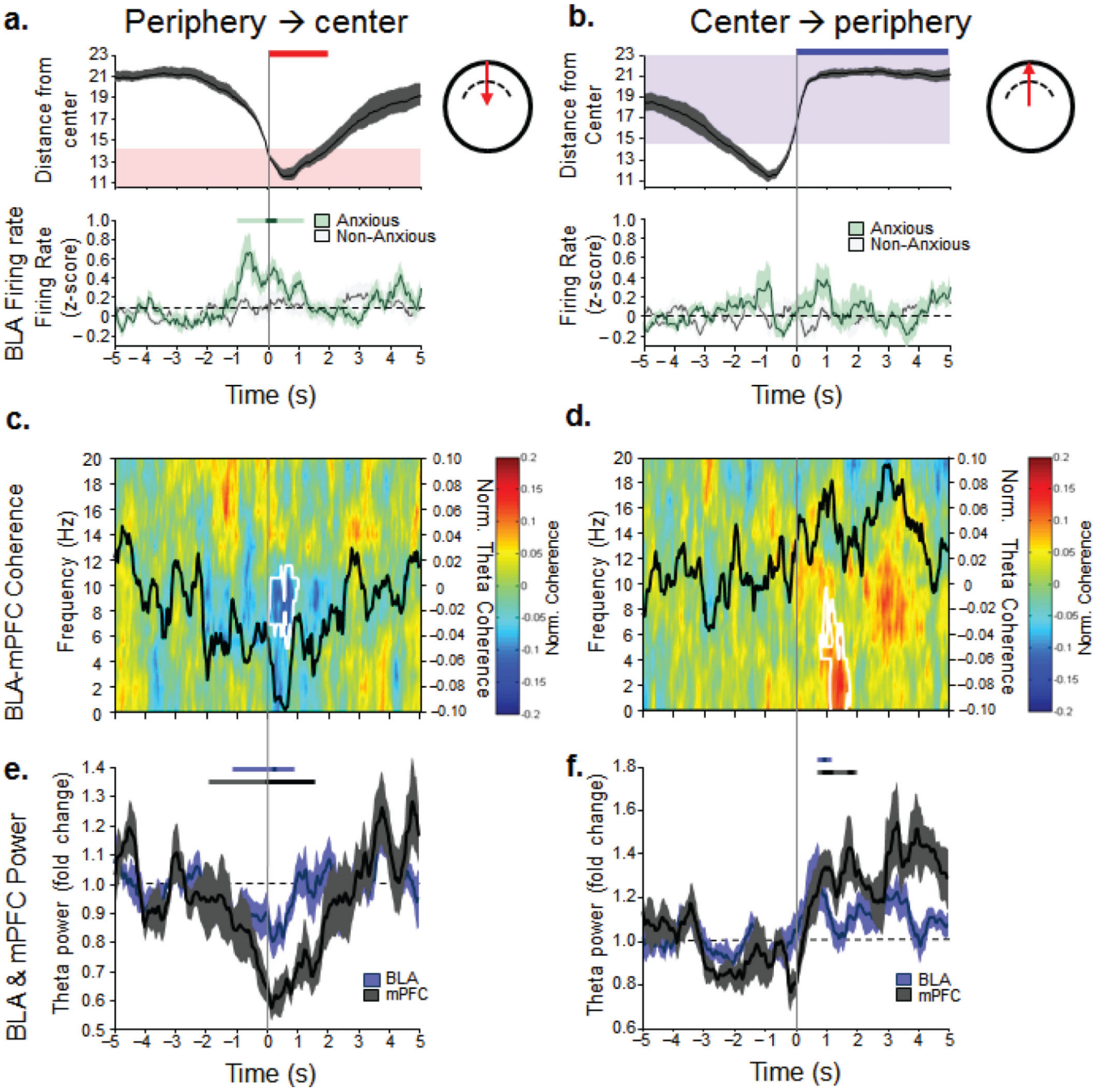

Figure 7. BLA-mPFC activity predicts center-periphery transitions of Anxious animals

(**a, b,** top panels), Animals' position during the transitions from the periphery to the center (left) and center to the periphery (right) as a function of time (transition occurred at zero, 5 seconds of data on both sides of the transition are shown). Red area, center of the open field, blue area, periphery of the open field. (**a,b**, bottom panels) Mean +/− sem (faded bands) BLA firing rate for Anxious and Non-anxious animals as they transition into (left) and out of (right) the center. Only the Anxious animals show a significant increase in BLA firing as they are going towards the center. +/−2 sec around transition point were compared to 3 sec

of baseline (−5 to −2s). Bonferoni-corrected ($p<.00042$ [$p<0.05/120$]) significant bins were identified (darker significance line). All time bins adjacent to the point-wise significant bins were tested for global significance ($p<0.05$, lighter significance lines), see Statistics. (**c,d**) Anxious animals: BLA-mPFC coherograms as the animals are entering the center (**c**) or the periphery (**d**). Black line, average theta coherence during the transitions, white contours, ranksum $p<0.05$, comparing +/−2 sec around transition point to baseline (**e,f**) Anxious animals: mean theta power BLA and mPFC +/− sem (faded bands) during transitions into (**e**) and out of (**f**) the center. Darker significance lines show point-wise significance (signrank, $p<.0039$) for at least two consecutive bins, lighter significance lines, globally significant (signrank, $p<.05$) bins adjacent to the point-wise significant bins (see Statistics).

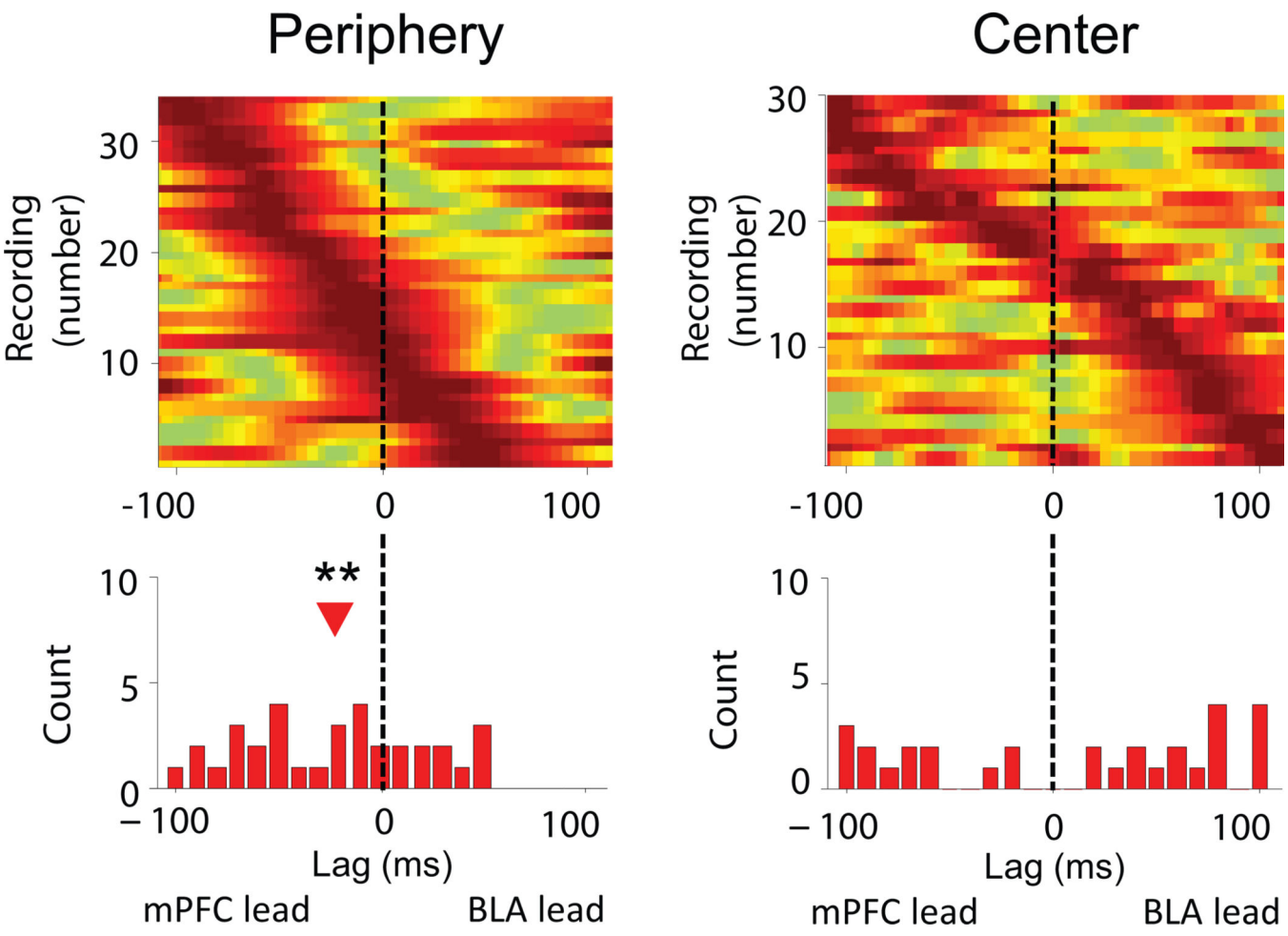

Figure 8. mPFC-to-BLA directionality in Anxious animals predicts safety in a test of innate anxiety

Strength of phase-locking of BLA MUA to mPFC theta oscillations as a function of lag in the periphery (right) and center (left) of the open field in Anxious animals. Conventions as in Figure 4d.